ACS APPLIED MATERIALS & INTERFACES

Forum Article

www.acsami.org

Sulfur-Functionalized Mesoporous Carbons as Sulfur Hosts in Li–S Batteries: Increasing the Affinity of Polysulfide Intermediates to Enhance Performance

Kimberly A. See,[†,‡,§] Young-Si Jun,[†,‡] Jeffrey A. Gerbec,[†,⊥] Johannes K. Sprafke,[†] Fred Wudl,[†,#] Galen D. Stucky,[†,‡,§,#] and Ram Seshadri*[,†,‡,§,#]

[†]Mitsubishi Chemical Center for Advanced Materials, [‡]Department of Chemistry and Biochemistry, [§]Materials Research Laboratory, and [#]Materials Department, University of California, Santa Barbara, California 93106, United States

[⊥]Mitsubishi Chemical USA, Inc., Chesapeake, Virginia 23320, United States

Supporting Information

ABSTRACT: The Li–S system offers a tantalizing battery for electric vehicles and renewable energy storage due to its high theoretical capacity of 1675 mAh g^{-1} and its employment of abundant and available materials. One major challenge in this system stems from the formation of soluble polysulfides during the reduction of S_8, the active cathode material, during discharge. The ability to deploy this system hinges on the ability to control the behavior of these polysulfides by containing them in the cathode and allowing for further redox. Here, we exploit the high surface areas and good electrical conductivity of mesoporous carbons (MC) to achieve high sulfur utilization while functionalizing the MC with sulfur (S–MC) in order to modify the surface chemistry and attract polysulfides to the carbon material. S–MC materials show enhanced capacity and cyclability trending as a function of sulfur functionality, specifically a 50% enhancement in discharge capacity is observed at high cycles (60–100 cycles). Impedance spectroscopy suggests that the S-MC materials exhibit a lower charge-transfer resistance compared with MC materials which allows for more efficient electrochemistry with species in solution at the cathode. Isothermal titration calorimetry shows that the change in surface chemistry from unfunctionalized to S-functionalized carbons results in an increased affinity of the polysulfide intermediates for the S–MC materials, which is the likely cause for enhanced cyclability.

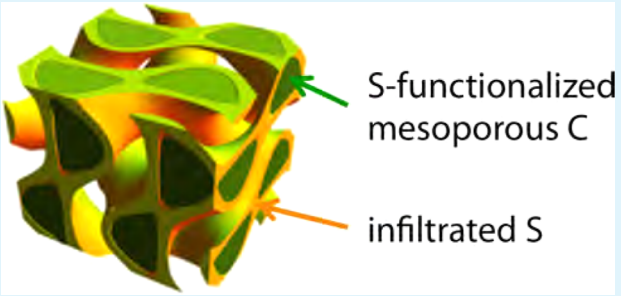

KEYWORDS: *lithium–sulfur cell, sulfur-functionalized porous carbons, isothermal titration calorimetry, sulfur cathode, enhance polysulfude affinity, mesoporous carbons*

INTRODUCTION

The increasing need for widely available clean energy technologies such as electric vehicles and renewable electricity generation require high-capacity energy storage systems utilizing abundant materials. Battery systems available for this kind of energy storage include intercalation and conversion reaction systems. The energy density and gravimetric capacity of intercalation strategies are limited by the heavy host lattices required for topotactic Li-ion intercalation. This mechanism fundamentally limits the capacity of intercalation materials to around 300 mAh g^{-1}, making them poor choices for lightweight batteries. Alternatively, conversion reaction battery systems can achieve the large gravimetric capacities necessary for lightweight batteries and open the door for the utilization of abundant resources.

The Li–S conversion reaction battery has one of the highest theoretical gravimetric capacities, making it an excellent system to study for lightweight batteries. The Li–S cell utilizes sulfur as the active cathode material, an ideal material for two main reasons. First, sulfur is highly abundant and not geographically isolated.[1] Second, the S atom can store two electrons yielding theoretical capacities of 1675 mAh g^{-1}, more than five times higher than the intercalation cells. Sulfur has its challenges, as well, which originate from its low electrical and ionic conductivities,[2] two very important properties for a battery material. These weaknesses necessitate the incorporation of conductive additives in the cathode, usually carbons, to facilitate electron transfer to the sulfur, as well as the use of electrolytes that slightly solubilize sulfur, allowing it to combine with the Li^+ and mitigating its low ionic conductivity.

Although the poor electrical and ionic conductivities can be improved by additives, the Li–S system in practice still shows poor cyclability, insufficient utilization of active material, and

Special Issue: New Materials and Approaches for Electrochemical Storage

Received: November 14, 2013
Accepted: February 4, 2014
Published: February 13, 2014

 © 2014 American Chemical Society dx.doi.org/10.1021/am405025n | *ACS Appl. Mater. Interfaces* 2014, 6, 10908–10916

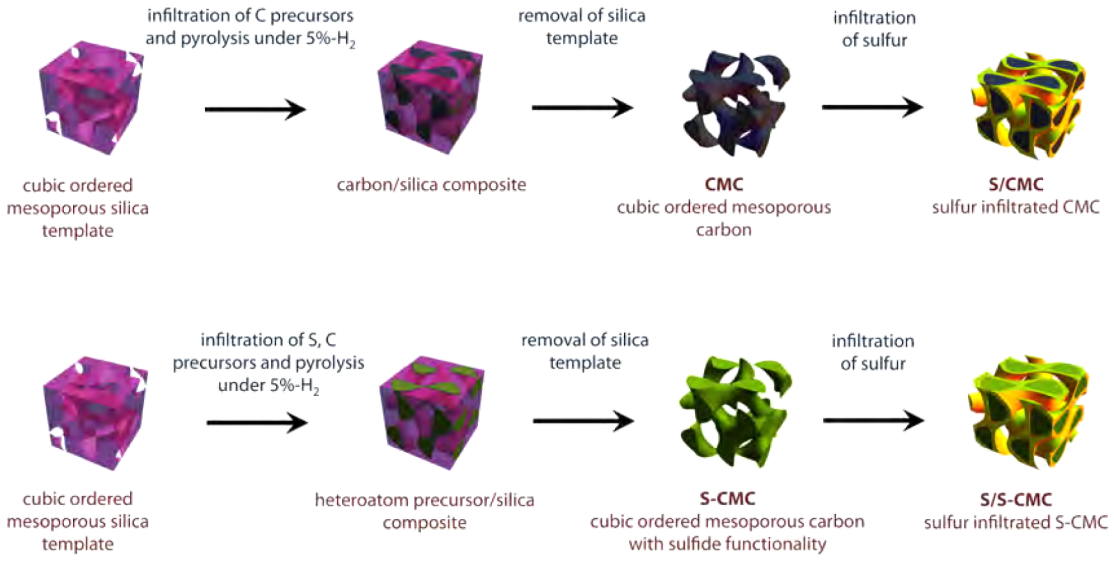

Figure 1. Preparation of cubic ordered mesoporous carbon (CMC) materials with and without sulfide functionality.

stability issues. The primary cause for these performance problems is the formation of intermediate polysulfide species formed during discharge. The long-chain polysulfides are soluble in the electrolyte leading to dissolution into the bulk electrolyte,[3,4] loss of active mass during every discharge, a steady fade in discharge capacity as the cell cycles, and parasitic side reactions of the polysulfides with the anode.[5]

Various efforts have been made to decrease the polysulfide dissolution by modifying nearly every aspect of the cell. For instance, Fu et al. found that a carbon fiber trap between the cathode and separator is able to trap polysulfides and prevent their migration to the anode.[6] Modification of the conductive carbon matrix in the cathode itself has also been shown to hold polysulfides in the cathode. Studies have evaluated graphene-wrapped sulfur[7] and sulfur–graphene composites,[8] sulfur-coated multiwalled carbon nanotubes sandwiched between graphene sheets,[9] hollow carbon nanofiber–encapsulated sulfur,[10] carbon sphere micropore-encapsulated sulfur,[11] sulfur–impregnated carbon nanotubes,[12] sulfur–impregnated activated carbon cloth,[13] and even sulfur–impregnated porous carbon derived from crab shells,[14] to name a few. Another interesting approach evaluated ordered mesoporous carbon (OMC) materials which exhibit high sulfur utilization due to their high specific surface areas (around 1000 m^2/g) which provide good electrical contact to the sulfur.[15] Since the first report utilizing OMCs as sulfur hosts by Ji et al. in 2009, several additional modifications to the OMC materials have been investigated. For example, hierarchically structured OMC,[16] bimodal OMC materials,[17] and OMC nanospheres[18] have been evaluated. These studies focus on modifying the structure of the pore network including the pore sizes or the size of the porous particles themselves.

We evaluate similar ordered mesoporous carbon materials and find that while the capacity decay is abated, additional modification of the pore network is needed to create a more amiable environment within the cathode for the polysulfides. Our work focuses on a compositional modification of the carbon material through the incorporation of sulfur functionalities, which are known to effect catalytic and capacitive behavior,[19−21] into the carbon materials. We find that the sulfur functionality changes the surface chemistry of the carbons resulting in enhanced affinity of intermediate polysulfides to the carbons and better cycling behavior.

Functionalizing the mesoporous carbons with sulfur functionality allows the cathode to better retain polysulfides in the mesoporous carbons (Figure 1). This modification increases the polarizability of the carbon material and could allow for S−S interactions between the S-functionalized carbon and the solubilized intermediate polysulfide materials. Here, we describe (1) the effect of the sulfur functionality (denoted by S), even in small weight fractions relative to the mesoporous carbon weight, on the capacity retention of the Li−S cell, and (2) the mechanism by which the S-functionalized carbons interact with a model lithium polysulfide solution.

EXPERIMENTAL SECTION

Materials Preparation. All mesoporous carbon materials were prepared via a hard templating method using mesoporous silica as the template. Both hexagonal and cubic ordered mesoporous carbons were prepared using the appropriately ordered mesoporous silica structure.

Hexagonal ordered mesoporous silica (SBA-15)[22] and cubic ordered mesoporous silica (KIT−6)[23] were prepared following the previously published routes. SBA-15 was prepared by dissolving Pluronic P123 block copolymer in diluted HCl (2 M). Tetraethylorthosilicate was then added while stirring. The solution was stirred at 38 °C for 6 min and allowed to rest for 24 h with no stirring. The solution was then heated to 100 °C in a Parr pressure vessel for 24 h. The resulting silicate was filtered and washed with ethanol and water and then calcined at 550 °C for 4 h in air. To achieve the cubic ordered mesoporous silica, we added butyl alcohol to the initial 2 M HCl solution at a 1:1 ratio with the P123.

The hexagonal ordered mesoporous carbons were templated with SBA-15 following previously published procedures.[22] Sucrose (0.86 g) was dissolved in water (3.5 mL) along with H_2SO_4 (0.1 g). The sucrose solution was then stirred with SBA-15 (0.7 g) and heated to 100 °C for 24 h to remove the water. The same procedure was followed for a second infiltration with 0.5 g sucrose. The sucrose/silica composite was then reduced in a tube furnace with flowing 5% H_2/Ar at 900 °C for 6 h. The silica template was removed by stirring in HF (24%) overnight. The resulting carbons were then filtered and washed with alternating 20 mL aliquots of ethanol and water until the filtrate reached about 150 mL. The carbon was then dried at 65 °C overnight. All silica templates were removed in this way.

Cubic ordered mesoporous carbons were prepared similarly following previously published procedures.[24,25] Boric acid (0.9 g)

was dissolved along with sucrose (0.6 g) and H_2SO_4 (17.8 M, 39 μL) to about 3 mL of water. We found that adding the boric acid helped to replicate the silica template pore network for our setup. The KIT−6 silica template (0.5 g) was stirred into the solution and subsequently placed in a sealed vessel and heated at 100 °C for1 h prior to removing the water. The composite was placed in an oven at 160 °C overnight. A second infiltration was done with sucrose (0.4 g), boric acid (0.9 g), and H_2SO_4 (17.8 M, 25.5 μL) in 2.7 mL of water. The composite was reduced at 900 °C under 5% H_2/Ar for 6 h. The boric acid phase separates into the silica during carbonization forming boron oxide and borosilicate and expands the pore size as described previously.[24] The silica template along with the boron oxide and borosilicate were then removed as described above.

The preparation of S-functionalized mesoporous carbons was inspired by previous work preparing sulfur-containing mesoporous carbon materials by Shin et al.[26] and Valle-Vigón et al.[27] Two methods were used to obtain a varying degree of sulfur-functionality in the mesoporous carbons. Cubic mesoporous silica, KIT-6, was used as the template for all S-functionalized materials. For the lowest wt% S material, *p*-toluenesulfonic acid monohydrate (PTSA, 0.62 g) was first dissolved in acetone (about 1 mL). KIT-6 (0.5 g) was stirred into the solution for 1.5 h. The acetone was removed and the resulting composite was heated at 100 °C overnight and then at 160 °C for 8 h. A second infiltration was done with PTSA (0.413 g) dissolved in about 7 mL of acetone following the same procedure. The material was then reduced at 900 °C under 5% H_2/Ar for 3 h. The silica template was removed as described above.

For the higher wt % S-containing mesoporous carbon, thiophene methanol was polymerized within the KIT-6 via an acid catalyzed polymerization, similar to the procedure described by Shin et al.[26] First, KIT-6 (0.48 g) was functionalized with PTSA (0.66 g) dissolved in acetone (about 1.5 mL). After removing the acetone, 2-thiophenemethanol (0.96 g) dissolved in toluene (4 mL) was added to the KIT-6 and stirred for 1.5 h until brown. The excess solvent was decanted and material was rinsed with additional toluene to remove any unreacted monomer. The material was then dried in a vacuum oven at 50 °C overnight. The resulting composite was reduced in a tube furnace with flowing 5% H_2/Ar at 800 °C for 4 h and the silica template was removed as previously described.

Materials Characterization. All porous materials were characterized by low-angle X-ray diffraction (XRD) and wide-angle XRD on a Scintag X2 $\theta-\theta$ diffractometer and Philips X'PERT MPD, respectively. N_2 sorption isotherms were measured on a MicroMeritics TriStar Porosimeter at 77 K. The materials were first degassed with flowing N_2 at 100 °C for 2 h followed by 200 °C for at least 10 h. Elemental analysis was performed on the materials to determine the wt % of C, H, and N using an automated organic elemental analyzer. The S content of the materials was determined by ^{34}S isotope ratio mass spectrometry. X-ray photoelectron spectroscopy (XPS) was done on a Kratos Axis Ultra X-ray Phototelectron Spectroscopy system with powders. The reduced C (284.8 eV) signal was used as the reference binding energy.

Isothermal titration calorimetry (ITC) was done on a TA Instruments Nano Isothermal Titration Calorimeter at 25 °C. Titration volumes were 10 μL with a relaxation time of 800 s between titrations and a stir rate of 350 rpm. Sample preparation was performed under Ar; however, loading the samples into the ITC required brief exposure to air (while in solution). ITC experiments were done in 1,3-dioxolane (a common Li−S electrolyte solvent). Ethyl methyl sulfone (EMS) is difficult to use for the ITC experiments as it is a solid at room temperature preventing the preparation of solutions with accurate concentrations. The "Li_2S_6" titrant solutions were prepared by reacting Li metal and S_8 in DOL by continuous mixing at 85 °C for 5 days in a sealed vessel under Ar. The initial solution was prepared at 5 M and subsequently diluted to obtain the various concentrations used for ITC. The heat of dilution of "Li_2S_6" in DOL was first determined by titrating the "Li_2S_6" solutions into DOL (see the Supporting Information, Figure S1). This background heat of dilution was subsequently subtracted titration by titration from all measurements thereafter.

Cell Assembly and Electrochemical Analyses. Prior to cell assembly, the CMC materials were first infiltrated with sulfur at 70% of the available pore volume (as determined by N_2 sorption analysis). The CMCs were ground with an agate mortar and pestle with the appropriate amount of precipitated sulfur. The powder was then placed in a Parr pressure vessel to prevent loss of sulfur during heating and then placed into an oven at 155 °C for two hours. The cathode materials were evaluated in 2032 coin cells (MTI). Cell assembly was performed in an Ar filled glovebox from the negative case (anode) upward and pressed with a MTI Corporation hydraulic crimping machine to 1000 psi. The entire volume of the cell was filled with electrolyte (1 M LiTFSI in ethyl methyl sulfone, EMS) to mimic industrial battery fabrication. Etched polypropylene separators (25 μm thick, Celgard) cut into 19 mm diameter discs were used along with composite, drop cast cathodes. Cathode casts were prepared by drop casting 84% S/CMC, 8% Super P (TIMCAL) conductive carbon, and 8% polyvinylidene fluoride (PVDF, battery grade, Mitsubishi Chemical) binder in dry cyclopentanone on carbon coated aluminum foil. Cathode casts were allowed to dry overnight prior to loading them into the glovebox. Li metal (12 mm diameter) anodes were punched out of Li foil and scraped clean in an Ar glovebox. All cells were measured at room temperature.

Electrochemical measurements were performed on a Bio−Logic Variable Multichannel Potentiostat. Galvanostatic cycling and impedance measurements were performed in 2032 coin cells. Impedance measurements were performed from 1000 kHz to 10 mHz with an amplitude of 100 mV.

RESULTS AND DISCUSSION

Our interests in the mesoporous carbon materials initially concerned the effect of the structure of the pore network. We compared the performance of hexagonal ordered mesoporous carbon, denoted as HMC, and cubic mesoporous carbon, denoted as CMC (Figure 2). The characterization of these materials can be found in the Supporting Information of our previous work.[28] Upon cycling the sulfur infiltrated mesoporous

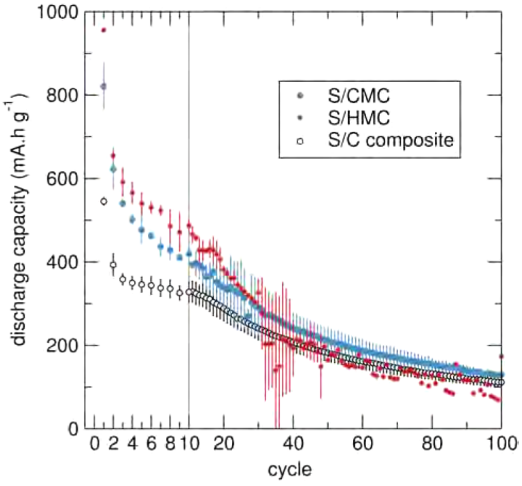

Figure 2. Galvanostatic discharge and charge curves of the sulfur infiltrated cubic ordered mesoporous carbon (S/CMC) materials vs hexagonally ordered mesoporous carbon materials (S/HMC). The cells are cycled at C/10 with 1 M LiTFSI in ethyl methyl sulfone electrolyte. The error bars represent the standard deviation of three replicate cells. The HMC cells tended to fail around 40 cycles which is indicated by the increase in the error bars when averaging the capacities. The data shown after 40 cycles with no error bars represents the one cell that was able to cycle. We believe this failure is due to the nature of the one-dimensional pore network afforded by the HMC.

carbons (denoted by S/HMC and S/CMC), the three-dimensionally connected pore network afforded by the CMC materials resulted in steadier cycling over 40 cycles. S/HMC cathodes continually failed at the higher cycle numbers. We believe that the isotropic pores of the HMC material clog more easily, resulting in a higher percentage of failed cells over 40 cycles. Because of the enhanced cyclability of the S/CMC materials, this pore network was selected as the baseline material to compare the effect of the S-functionality.

The polar nature of the polysulfide intermediates was the primary consideration when determining what kind of functionality would be most effective. The ionic nature of the polysulfides suggests that increasing the polarizability of the surface of the carbons would be an advantageous modification; however, this modification cannot negatively affect the surface area or the conductivity. By including a heteroatom in the carbon precursor material prior to pyrolysis, the nature of the mesoporous carbon can be modified without significantly reducing the conductivity and maintaining the pore structure of the template. Pyrolysis of the heteroatom precursor *p*-toluenesulfonic acid results in sulfur incorporation into the carbon. The chemical nature of the sulfur is discussed in the following paragraph. The material contains 3.2 wt % S and is denoted $S_{3.2}$-CMC. Simply using a heteroatom precursor such as thiophene, with a higher S:C ratio, does not produce a material with higher sulfur functionality in the resulting carbons due to the high pyrolysis temperature required to reduce carbon. Thiophene is lost due to its low boiling point leaving no material behind at the temperatures where carbonization occurs. An extended network must be prepared within the silica template prior to pyrolysis which contains an already thermally stable sulfide moiety, as in thiophene. With this in mind, the higher wt % S-CMC was prepared by polymerizing thiophenemethanol within KIT-6 yielding a mesoporous carbon material with 5.5 wt % S ($S_{5.5}$-CMC). The resulting carbons contain a cubic ordered pore system (Figure 3a) and retains its amorphous nature (Figure 3b) independent of the precursor. The high sulfur content material contains almost double the S content and a similar, although not identical, pore system (Figure 4). The BET surface areas for each material are

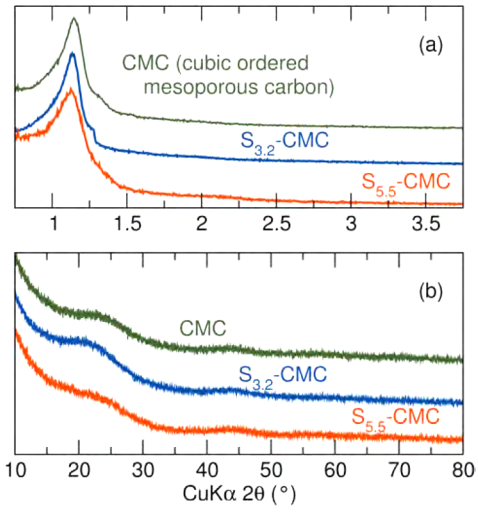

Figure 3. X-ray diffraction (XRD) of the cubic mesoporous carbon materials (CMC). The weight percent of sulfur functionality of the S-functionalized CMCs (S-CMC) is denoted by the subscript. (a) Small-angle XRD of the CMCs show the ordering of the pore structure independent of the precursor used for the CMCs. (b) Wide-angle XRD shows the two broad peaks centered around 21 and 45° 2θ, characteristic of amorphous carbon.

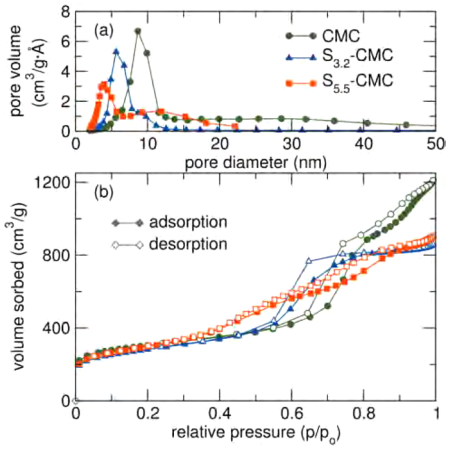

Figure 4. N_2 sorption analysis of the cubic mesoporous carbon materials (CMC). The weight percent of sulfur functionality of the S-functionalized CMCs (S-CMC) is denoted by the subscript. (a) The pore size distribution shows the majority of the pores to be mesoporous. The $S_{5.5}$-CMC material displays a smaller pore size making direct comparison of the materials difficult. (b) All materials show the characteristic Type IV isotherms indicative of mesoporous networks. The isotherms are not identical for each CMC indicating that the pore networks are slightly different.

above 1000 m^2/g allowing for good contact to the infiltrated sulfur. The BET surface area, pore volume, micropore surface area, and BJH pore size along with the elemental analysis of all the CMCs are tabulated in Table 1. By changing the precursor material, the pore system varies slightly across the series of materials. For instance, the average pore diameter for the $S_{5.5}$-CMC material is larger than $S_{3.2}$-CMC (Figure 4b). This pore size variability which coincidentally corresponds well with the sulfur content is probably not related to the sulfur functionality at all. By changing the carbon precursor used for the pyrolysis, the pyrolysis procedure will vary, resulting in different mass losses during pyrolysis and possibly even a variation in the temperature at which pyrolysis begins due to the different bond strengths of the precursor. Both precursors utilize largely already aromatic carbons, however, so the temperature is probably not a big factor. With careful manipulation of the infiltration and pyrolysis conditions, we expect that an identical pore structure would be obtainable even using varied carbon precursor material; however, we did not explore this aspect, as the focus of this paper was to obtain a high-surface-area cubic ordered mesoporous carbon with sulfur incorporation.

The XPS of the S-functionalized materials reveals that the sulfur is carbon bound in a thiophenic moiety. We see only sulfur, carbon, and oxygen in the sample and there is only one sulfur environment as evidenced by the single 2p doublet (Figure 5a). There is no evidence for any S−O environments that would show up above 166 eV[29] and elemental sulfur would not survive the pyrolysis conditions so the sulfur must be bound to carbon. The possible organosulfur compounds that would survive the pyrolysis conditions include thiophenic moieties consisting of an aromatic C−S−C type bond. Additionally, the position of the S $2p_{3/2}$ peak at 163.8 eV corresponds well with other sulfur-doped carbonaceous materials in which an aromatic C−S−C type bonding is

Table 1. Pore Network and Composition of Cubic Mesoporous Carbon (CMC) Materials from N_2 Sorption Analysis and Elemental Analysis

					elemental analysis (wt%)			
material	BET surface area (m^2/g)[a]	pore volume (cm^3/g)[b]	micropore surface area (m^2/g)[c]	BJH pore size (nm)	C	H	N	S
CMC	1046	1.8	479	9.5	74.2	0.8	0.2	
$S_{3.2}$-CMC	1176	1.6	350	5.9	89.8	1.3	0.3	3.2
$S_{5.5}$-CMC	1044	1.4	249	5.0	88.9	1.5	0.3	5.5

[a]Multipoint surface area calculated from the adsorption branch between $0.1p/p_o$ and $0.25p/p_o$. [b]Single point pore volume from the desorption branch at $0.98p/p_o$. [c]Calculated using the t-plot method.

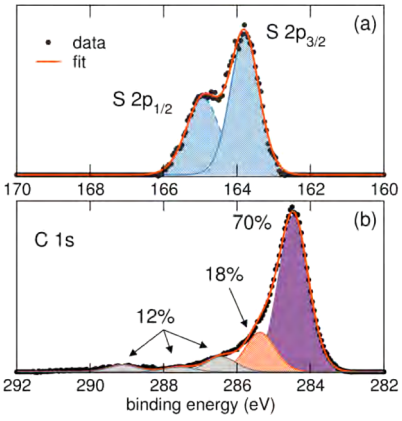

Figure 5. XPS of S-CMC shows (a) the S $2p_{1/2}$ and the S $2p_{3/2}$ can be fit by a single set of doublets indicating that there is a single chemical environment for S. The S $2p_{3/2}$ peak position corresponds well to carbon bound sulfur. (b) The C 1s envelope is defined well by 5 separate environments. The majority of the surface C (70%) exhibits a peak at very low binding energy indicating a graphitic-type carbon while 18% of the surface C is probably bound to sulfur. The three peaks above 286 eV correspond to oxidized surface states.

suggested.[19,20] The carbon 1s peak can be fit with 5 constituent peaks with a full width at half-maximum of 0.96 eV corresponding to the various carbon environments present in the amorphous carbon material (Figure 5b). It is not immediately obvious which peak corresponds to carbon-bound sulfur. The carbon environments above 286 eV can, however, be assigned to oxidized surface states which are always present on the surface of amorphous carbon materials and could include carbonyls, ethers, carboxylic acids, etc.[30] The two lower binding energy peaks are more interesting. The lowest peak corresponds to graphite-like carbon, whereas the peak at 285.4 eV could either be carbon bound sulfur or aliphatic-like carbon that shows up in carbon blacks.[30] At pyrolysis temperatures above 700 °C, however, the aliphatic carbon peak should constitute less than 5% of the total carbon environments.[30] These carbons are pyrolyzed at 900 °C suggesting that most of the reduced carbon should show up at the low binding energies, however, we still see a significant peak at slight higher binding energies of 285.4 eV. This peak is 18% of the carbon environment, which is much higher than we would expect for aliphatic carbon contributions, suggesting that this peak probably corresponds to the C−S environment.

The ability of the S-CMC material to retain polysulfides was determined by cycling sulfur infiltrated CMCs (at 70% of the available pore volume) vs a Li anode (Figure 7b) in 1 M LiTFSI in ethyl methyl sulfone (EMS) electrolyte. This electrolyte was chosen for the cycling experiments because it is known that soluble polysulfides are formed during discharge[4] allowing for the evaluation of the interaction between S-functionalized CMCs with solubilized polysulfides. The performance of S/CMC was established as a baseline to compare capacities and capacity fade. All cells exhibit the characteristic Li−S discharge and charge profiles with two distinct plateaus on the discharge and a long, single plateau on the charge (Figure 6). The absence of additional structure in

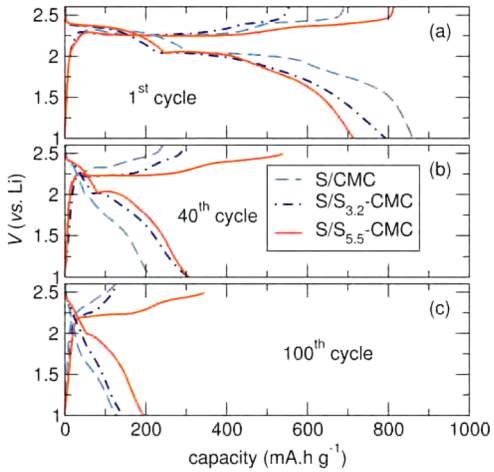

Figure 6. Galvanostatic discharge and charge curves of the sulfur infiltrated cubic ordered mesoporous carbon (S/CMC) materials with and without sulfur functionality for the (a) 1st cycle, (b) 40th cycle, and (c) 100th cycle. The wt % sulfur functionality is denoted by $S_{\#}$-CMC. The cells are cycled at $C/10$ between 1.0 and 2.6 V with 1 M LiTFSI in ethyl methyl sulfone electrolyte and show the characteristic Li−S plateaus. The $S_{5.5}$-CMC material shows higher charge capacities, especially at higher cycles which allows for higher subsequent discharge capacities. The charge capacities are higher due to favorable interactions between the solubilized polysulfides and the $S_{\#}$-CMC. The consequence of these favorable interactions are enhanced at higher cycles becaues of the increasing concentration of polysulfides as the cell cycles.

the profiles suggest that the sulfur functionality itself is not participating in the discharge or charge. This is confirmed by the negligible capacity observed when cycling S-CMCs in the absence of infiltrated sulfur (see the Supporting Information, Figure S2).

The high surface areas of the mesoporous materials increase the electrical contact to insulating sulfur and result in much higher initial discharge capacities compared to a composite of sulfur with conductive carbon (Super P). The S/CMC material, containing no sulfur functionality, exhibits a steady capacity fade as the cell cycles. Just 3.2 wt % sulfide functionality results in a lesser capacity fade; however, at higher cycle numbers (>80 cycles), the cell cycles very similarly to the neat CMC (Figure 7a). To maintain capacity retention above 80 cycles, a higher degree of sulfur functionality is required. The $S_{5.5}$-CMC

material steadily outperforms the CMC material by 50% over 60 cycles. This trend can be seen more clearly when the capacities are plotted normalized to the neat CMC material (S/CMC) (Figure 7b).

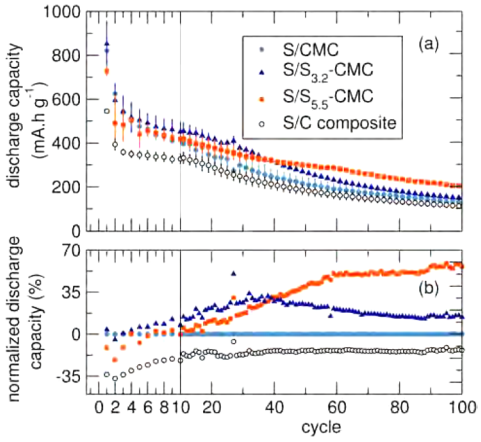

Figure 7. Galvanostatic cycling of the sulfur infiltrated cubic ordered mesoporous carbon (S/CMC) materials with and without sulfide functionality. The wt % sulfur functionality denoted by $S_{\#}$-CMC. The cells are cycled at C/10 with 1 M LiTFSI in ethyl methyl sulfone electrolyte. (a) The discharge capacities as a function of cycle number show enhancement sulfur utilization (capacity) provided by the mesoporous materials as a result of their high surface area. Error bars indicate the standard deviation of 3 replicate cells. The S-functionalized CMC materials show enhanced capacity retention. (b) The effect of sulfur functionality is more clearly demonstrated when the discharge capacities are normalized to the unfunctionalized CMC. The discharge capacities normalized to the unmodified CMC are plotted vs cycle number. The $S_{5.5}$-CMC shows a 55% increase in capacity after 100 cycles.

Capacity retention is improved as sulfur functionality is introduced into the mesoporous carbon materials even though the S-CMC materials show slightly lower capacities initially. The initial low capacity is probably due to the slightly lower conductivity of the S-CMCs, as shown by the increase in impedance of the S-CMC cells prior to cycling (Figure 8a). The discharge capacity for the first cycle of S/$S_{5.5}$-CMC is much lower than the other two CMCs because of the slight decrease in conductivity. However, at the high cycle numbers, S/$S_{5.5}$-CMC outperforms the other materials because of the functionality.

Electrochemical impedance spectroscopy (EIS) was measured on the cells before cycling and at a fully charged state after cycling in order to gain insight into the mechanism by which sulfur functionality helps retain capacity (Figure 8). The Nyquist plots are relatively similar before cycling but the S−CMCs show dramatically different responses after cycling compared to the CMC material. Qualitatively speaking, a dramatic increase in the diameter of the first semicircle at high frequencies is observed for the CMC materials. This semicircle corresponds to the charge-transfer behavior of the electrodes.[31] The decreased width of the semicircle exhibited by the S-CMC materials after cycling suggests that the charge-transfer impedance is greatly subdued.

The EIS spectra are fit to the equivalent circuit shown in Figure 8 to allow for quantitative comparisons of the resistance elements. The proposed circuit has been used previously to describe Li−S cells.[32] Constant phase elements (CPE) are used

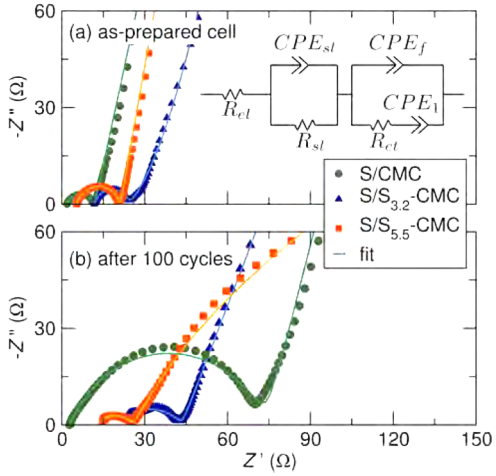

Figure 8. Electrochemical impedance spectroscopy of the cells with the various sulfur hosts (a) before and (b) after cycling. The symbols represent the data and each fit overlaid as a solid line. The inset circuit represents the equivalent circuit for the fits. The tabulated values for the fit can be found in Table 2. The S-CMC materials initially show slightly higher impedance probably due to a difference in conductivity of the carbon materials. After cycling, S/CMC cell shows much higher impedance compared with the S/S-CMC cells. The maximum $-Z''$ for the first semicircle in the as-prepared state for S/CMC, S/$S_{3.2}$-CMC, and S/$S_{5.5}$-CMC occur at 2454, 3630, and 2020 Hz, respectively. The maximum $-Z''$ for the first semicircle in the cycled state for S/CMC, S/$S_{3.2}$-CMC, and S/$S_{5.5}$-CMC occur at 239, 11562, and 54562 Hz, respectively.

in place of capacitance elements. Capacitance elements are not ideal for our system because of the roughness of the particle surfaces, an effect intrinsic to using powders, which results in imperfect semicircles with centers below the *x*-axis in the Nyquist plot. These elements are better modeled by CPEs.[32,33] The impedance corresponding to the diffusion of Li^+ at the solid−electrolyte interface has been modeled by either a CPE[32] or a Warburg element. We use a CPE to model this element because Warburg impedance exhibits a signature 45° line at low frequencies and this is not evident in our Nyquist plots. The physical explanation of each resistance element in the equivalent circuit is: R_{el} is the bulk ohmic resistance, which is dominated by the electrolyte but also includes the resistance of the electrodes; R_{sl} corresponds to the resistance of the surface layers on both the anode and cathode; R_{sl} is in parallel with CPE_{sl}, the capacitance of the surface layers, R_{ct} corresponds to the charge transfer resistance at the carbon/electrolyte interface, CPE_f is the capacitance of the carbon material, and CPE_1 models the diffusion of the polysulfides.

After cycling, the S-CMC materials show higher R_{sl} values and much lower R_{ct} values compared to the unfunctionalized CMC (Table 2). Higher R_{sl} values indicate that the surface layers formed on the S-CMC materials are more insulating than

Table 2. Resistance Values Obtained by Fitting the Nyquist Plots in 8 to the Inset Equivalent Circuit

	as-prepared/after 100 cycles		
	R_{el} (Ω)	R_{sl} (Ω)	R_{ct} (Ω)
S/S-CMC	1.76/0.28	9.94/2.46	8.71/72.0
S/$S_{3.2}$-CMC	9.31/16.2	38.6/17.6	8.02/9.85
S/$S_{5.5}$-SMC	5.35/13.0	15.6/479	33.8/11.9

dx.doi.org/10.1021/am405025n | ACS Appl. Mater. Interfaces 2014, 6, 10908−10916

the surface layer formed on the CMC material. The surface layers are likely oxidized sulfur in all cases as this is the well-known insulating solid charge product. The EIS data suggest that perhaps the S-CMC materials allow for more sulfur deposition resulting in an increase in the resistance of the surface layer and higher R_{sl} values. This would suggest that the S-CMC materials allow for enhanced oxidation efficiency of the dissolved polysulfide species. This can be seen directly by the much higher capacity exhibited at the 100th cycle by the S-CMC materials compared to that of the CMC materials. $S_{5.5}$-CMC materials exhibit a charge capacity of 350 mAh g^{-1}, whereas CMC shows 100 mAh g^{-1}. Concurrently, the lower R_{ct} values are likely a result of the S-functionality decreasing the interfacial resistance between the carbon surface and the dissolved polysulfides. The ability of the S-CMC materials to attract polysulfides to the surface of the carbons results in higher concentrations of polysulfides in the mesoporous material and thus decreases the charge transfer resistance. This interaction will be probed further using isothermal titration calorimetry later in this paper. Low charge transfer resistance allows for more efficient electrochemical reactions at the cathode.[31,32]

The EIS data imply that the charge transfer resistance between S-functionalized CMC and the dissolved polysulfides is much lower compared to the neat CMC. To evaluate this behavior, we explored the interaction of intermediate polysulfides with the CMCs directly through calorimetry. Isothermal titration calorimetry (ITC) is a good tool to explore surface interactions as it can detect heats as low as 0.05 μJ. Although this technique is most commonly used for aqueous solutions, there have been prior reports of using ITC in organic solvents and with suspensions.[34] For our purposes, ITC allows for the qualitative determination of thermodynamic differences between the intermediate polysulfide materials interacting with CMC vs $S_{5.5}$-CMC. A solution of "Li_2S_6" in 1,3-dioxolane (DOL) represents the dissolved polysulfide species in the cell, which is titrated into a suspension of the mesoporous carbon materials. Interestingly, although the raw heats are exothermic (Figure 9a), once the background heat resulting from the dilution of the polysulfide solution as it is titrated into the sample cell is subtracted, the interaction between the "Li_2S_6" solution and unmodified carbons is clearly endothermic reaching values over 100 kJ mol^{-1} during the initial injections (Figure 9). When the sample cell contains S-CMCs, however, this significant endothermic response is strongly subdued. This suggests that the interaction between polysulfides and CMCs is less favorable than with the S-CMC materials and could be the reason for enhanced capacity retention exhibited by the S-CMCs during battery cycling.

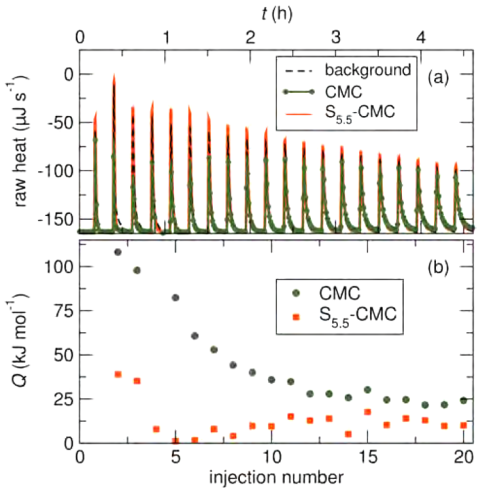

Figure 9. Isothermal titration calorimetry (ITC) on suspensions of the mesoporous carbon materials in 1,3-dioxolane. The titrant solution is 6.786 mM "Li_2S_6" in DOL intended to simulate dissolved polysulfide species. (a) Heat evolved (exotherm is upwards) upon a 10 μL titration of 6.786 mM "Li_2S_6" in DOL into a suspension of mesoporous carbons (1.03 mg L^{-1} CMC and 1.04 mg L^{-1} $S_{5.5}$-CMC to maintain a constant surface area in the sample cell). The background heat of dilution measured by titrating the same titrant solution into DOL alone is also shown. (b) The integrated heat of interaction (per mole of titrant) between the polysulfides and the CMCs show that the unmodified CMCs show an endothermic response once the background heat of dilution is subtracted. This unfavorable response is greatly subdued with the addition of S-functionality. This indicates that the polysulfides interact with the $S_{5.5}$-CMC more favorably thermodynamically.

CONCLUSIONS

The sulfur functionality in the mesoporous carbons enhances the cyclability of the cell because of a decreased repulsion between the polysulfide species and the surface of the modified mesoporous carbons. Because of the relatively low heats observed when the polysulfide species are titrated into the S-CMC materials, we believe this interaction is not due to bond formation between the S-functional groups in the CMCs and the polysulfides. Rather, this interaction is more akin to "hydrophilic" vs. "hydrophobic" interactions where the polysulfide species are driven away from the unmodified carbon materials because of unfavorable thermodynamic interactions, whereas these unfavorable interactions are greatly subdued when the polarizability is increased and the nature of the surface is changed by introducing the sulfur-functionality. The effect of this functionality can be seen as the cell is cycled and in the electrochemical impedance spectroscopy as the charge transfer resistance is much lower for the S-CMC materials. At cycle numbers greater than 10, when more of the active cathode material exists as polysulfides, the S-CMC materials exhibit much higher capacities. Between cycles 60 and 100, the $S_{5.5}$-CMC materials reproducibly exhibit capacities 50% higher than unmodified the CMCs. Changing the surface chemistry of the CMCs greatly improves polysulfide reactivity. We believe this modification is not limited to sulfur incorporation but it can be achieved through many routes such as the inclusion of heteroatoms such as N or P. In fact, N-doped carbons have very recently been shown to improve the Li–S cell performance compared to undoped carbons and we suggest that this is due to an increase in affinity of the polysulfides to the doped carbon.[35,36] Additionally, this is the first time, to the best of our knowledge, that ITC has been used to evaluate the interaction of the soluble polysulfides with the cathode structure. This technique can be very useful in evaluating effective polysulfide trapping materials without ever cycling the material in a cell. We are currently evaluating this technique further in order to directly quantify the enthalpy of interaction between various materials and polysulfide solutions.

ASSOCIATED CONTENT

Supporting Information

Heat of dilution of "Li_2S_6" solutions at concentrations of 4.865 and 6.786 mM, cyclic voltammetry and galvanostatic cycling of S-CMC materials with and without S infiltration. This material

is available free of charge via the Internet at http://pubs.acs.org/.

AUTHOR INFORMATION

Corresponding Author

*E-mail: seshadri@mrl.ucsb.edu.

Notes

The authors declare no competing financial interest.

ACKNOWLEDGMENTS

We thank Georges Paradis and William Clinton for assistance with CHN analysis and ^{34}S isotope analysis. We thank Dr. Tomohiro Kawai of Mitsubishi Chemical for helpful discussions on electrochemical methods. Fellowship support to KAS from the ConvEne IGERT Program of the National Science Foundation (DGE 0801627) is gratefully acknowledged. This research made extensive use of the shared experimental facilities of the Materials Research Laboratory (MRL). The MRL Shared Experimental Facilities are supported by the MRSEC Program of the NSF under Award DMR 1121053; a member of the NSF-funded Materials Research Facilities Network (www.mrfn.org).

REFERENCES

(1) Gaultois, M. W.; Sparks, T. D.; Borg, C. K. H.; Seshadri, R.; Bonificio, W. D.; Clarke, D. R. Data-Driven Review of Thermoelectric Materials: Performance and Resource Considerations. *Chem. Mater.* **2013**, *25*, 2911−2920.

(2) Ellis, B. L.; Lee, K. T.; Nazar, L. F. Positive Electrode Materials for Li−Ion and Li−Batteries. *Chem. Mater.* **2010**, *22*, 691−714.

(3) Rauh, R.; Shuker, F.; Marston, J.; Brummer, S. Formation of Lithium Polysulfides in Aprotic Media. *J. Inorg. Nucl. Chem.* **1977**, *39*, 1761−1766.

(4) Dominko, R.; Demir-Cakan, R.; Morcrette, M.; Tarascon, J.-M. Analytical Detection of Soluble Polysulphides in a Modified Swagelok Cell. *Electrochem. Commun.* **2011**, *13*, 117−120.

(5) Mikhaylik, Y. V.; Akridge, J. R. Polysulfide Shuttle Study in the Li−S Battery System. *J. Electrochem. Soc.* **2004**, *151*, A1969−A1976.

(6) Fu, Y.; Su, Y.-S.; Manthiram, A. Highly Reversible Lithium/Dissolved Polysulfide Batteries with Carbon Nanotube Electrodes. *Angew. Chem., Int. Ed.* **2013**, *52*, 6930−6935.

(7) Wang, H.; Yang, Y.; Liang, Y.; Robinson, J. T.; Li, Y.; Jackson, A.; Cui, Y.; Dai, H. Graphene-Wrapped Sulfur Particles as a Rechargeable Lithium−Sulfur Battery Cathode Material with High Capacity and Cycling Stability. *Nano Lett.* **2011**, *11*, 2644−2647.

(8) Wang, J.-Z.; Lu, L.; Choucair, M.; Stride, J. A.; Xu, X.; Liu, H.-K. Sulfur-Graphene Composite for Rechargeable Lithium Batteries. *J. Power Sources* **2011**, *196*, 7030−7034.

(9) Chen, R.; Zhao, T.; Lu, J.; Wu, F.; Li, L.; Chen, J.; Tan, G.; Ye, Y.; Amine, K. Graphene-Based Three-Dimensional Hierarchical Sandwich-type Architecture for High-Performance Li/S Batteries. *Nano Lett.* **2013**, *13*, 4642−4649.

(10) Zheng, G.; Yang, Y.; Cha, J. J.; Hong, S. S.; Cui, Y. Hollow Carbon Nanofiber-Encapsulated Sulfur Cathodes for High Specific Capacity Rechargeable Lithium Batteries. *Nano Lett.* **2011**, *11*, 4462−4467.

(11) Zhang, B.; Qin, X.; Li, G. R.; Gao, X. P. Enhancement of Long Stability of Sulfur Cathode by Encapsulating Sulfur into Micropores of Carbon Spheres. *Energy Environ. Sci.* **2010**, *3*, 1531−1537.

(12) Guo, J.; Xu, Y.; Wang, C. Sulfur−Impregnated Disordered Carbon Nanotubes Cathode for Lithium−Sulfur Batteries. *Nano Lett.* **2011**, *11*, 4288−4294.

(13) Elazari, R.; Salitra, G.; Garsuch, A.; Panchenko, A.; Aurbach, D. Sulfur−Impregnated Activated Carbon Fiber Cloth as a Binder−Free Cathode for Rechargeable Li−S Batteries. *Adv. Mater.* **2011**, *23*, 5641−5644.

(14) Yao, H.; Zheng, G.; Li, W.; McDowell, M. T.; Seh, Z.; Liu, N.; Lu, Z.; Cui, Y. Crab Shells as Sustainable Templates from Nature for Nanostructured Battery Electrodes. *Nano Lett.* **2013**, *13*, 3385−3390.

(15) Ji, X.; Lee, K. T.; Nazar, L. F. A Highly Ordered Nanostructured Carbon-Sulphur Cathode for Lithium-Sulphur Batteries. *Nat. Mater.* **2009**, *8*, 500−506.

(16) Liang, C.; Dudney, N. J.; Howe, J. Y. Hierarchically Structured Sulfur/Carbon Nanocomposite Material for High−Energy Lithium Battery. *Chem. Mater.* **2009**, *21*, 4724−4730.

(17) He, G.; Ji, X.; Nazar, L. High "C″ rate Li−S cathodes: Sulfur Imbibed Bimodal Porous Carbons. *Energy Environ. Sci.* **2011**, *4*, 2878−2883.

(18) Schuster, J.; He, G.; Mandlmeier, B.; Yim, T.; Lee, K. T.; Bein, T.; Nazar, L. F. Spherical Ordered Mesoporous Carbon Nanoparticles with High Porosity for Lithium−Sulfur Batteries. *Angew. Chem., Int. Ed.* **2012**, *51*, 3591−3595.

(19) Yang, Z.; Yao, Z.; Li, G.; Fang, G.; Nie, H.; Liu, Z.; Zhou, X.; Chen, X.; Huang, S. Sulfur−doped Graphene as an Efficient Metal-free Cathode Catalyst for Oxygen Reduction. *ACS Nano* **2012**, *6*, 205−211.

(20) Wohlgemuth, S.-A.; White, R. J.; Willinger, M.-G.; Titirici, M.-M.; Antonietti, M. A One-pot Hydrothermal Synthesis of Sulfur and Nitrogen Doped Carbon Aerogels with Enhanced Electrocatalytic Activity in the Oxygen Reduction Reaction. *Green Chem.* **2012**, *14*, 1515−1523.

(21) Hasegawa, G.; Aoki, M.; Kanamori, K.; Nakanishi, K.; Hanada, T.; Tadanaga, K. Monolithic Electrode for Electric Double-layer Capacitors Based on Macro/meso/microporous S-Containing Activated Carbon with High Surface Area. *J. Mater. Chem.* **2011**, *21*, 2060−2063.

(22) Zhao, D.; Huo, Q.; Feng, J.; Chmelka, B. F.; Stucky, G. D. Nonionic Triblock and Star Diblock Copolymer and Oligomeric Surfactant Syntheses of Highly Ordered, Hydrothermally Stable, Mesoporous Silica Structures. *J. Am. Chem. Soc.* **1998**, *120*, 6024−6036.

(23) Kleitz, F.; Choi, S. H.; Ryoo, R. Cubic Ia3d Large Mesoporous silica: Synthesis and Replication to Platinum Nanowires, Carbon Nanorods and Carbon Nanotubes. *Chem. Commun.* **2003**, 2136−2137.

(24) Lee, H. I.; Kim, J. H.; You, D. J.; Lee, J. E.; Kim, J. M.; Ahn, W.-S.; Pak, C.; Joo, S. H.; Chang, H.; Seung, D. Rational Synthesis Pathway for Ordered Mesoporous Carbon with Controllable 30- to 100-Angstrom Pores. *Adv. Mater.* **2008**, *20*, 757−762.

(25) Dai, W.; Zheng, M.; Zhao, Y.; Liao, S.; Ji, G.; Cao, J. Template Synthesis of Three-Dimensional Ordered Mesoporous Carbon With Tunable Pore Sizes. *Nanoscale Res. Lett.* **2009**, *5*, 103−107.

(26) Shin, Y.; Fryxell, G. E.; Um, W.; Parker, K.; Mattigod, S. V.; Skaggs, R. Sulfur-Functionalized Mesoporous Carbon. *Adv. Funct. Mater.* **2007**, *17*, 2897−2901.

(27) Valle-Vigon, P.; Sevilla, M.; Fuertes, A. B. Functionalization of Mesostructured Silica−Carbon Composites. *Mater. Chem. Phys.* **2013**, *139*, 281−289.

(28) See, K. A.; Gerbec, J. A.; Jun, Y.-S.; Wudl, F.; Stucky, G. D.; Seshadri, R. A High Capacity Calcium Primary Cell Based on the Ca−S System. *Adv. Energy Mater.* **2013**, *3*, 1056−1061.

(29) Heeg, J.; Kramer, C.; Wolter, M.; Michaelis, S.; Plieth, W.; Fischer, W. J. Polythiophene−O_3 Surface Reactions Studied by XPS. *Appl. Surf. Sci.* **2001**, *180*, 36−41.

(30) Darmstadt, H.; Roy, C.; Kaliaguine, S. ESCA Characterization of Commercial Carbon Blacks and of Carbon Blacks from Vacuum Pyrolysis of Used Tires. *Carbon* **1994**, *32*, 1399−1406.

(31) Choi, Y.-J.; Chung, Y.-D.; Baek, C.-Y.; Kim, K.-W.; Ahn, H.-J.; Ahn, J.-H. Effects of Carbon Coating on the Electrochemical Properties of Sulfur Cathode for Lithium/Sulfur Cell. *J. Power Sources* **2008**, *184*, 548−552.

(32) Li, Y.; Zhan, H.; Liu, S.; Huang, K.; Zhou, Y. Electrochemical Properties of the Soluble Reduction Products in Rechargeable Li/S Battery. *J. Power Sources* **2010**, *195*, 2945−2949.

(33) Yuan, L.; Qiu, X.; Chen, L.; Zhu, W. New Insight into the Discharge Process of Sulfur Cathode by Electrochemical Impedance Spectroscopy. *J. Power Sources* **2009**, *189*, 127−132.

(34) Alston, J. R.; Overson, D.; Poler, J. C. Direct Measurement of the Interactions of Amide Solvents with Single-Walled Carbon Nanotubes using Isothermal Titration Calorimetry. *Langmuir* **2012**, *28*, 264−271.
(35) Zhou, L.; Lin, X.; Huang, T.; Yu, A. Nitrogen−doped Porous Carbon Nanofiber Webs/Sulfur Composites as Cathode Materials for Lithium−Sulfur Batteries. *Electrochim. Acta* **2014**, *116*, 210−216.
(36) Yang, J.; Xie, J.; Zhou, X.; Zou, Y.; Tang, J.; Wang, S.; Chen, F.; Wang, L. Functionalized N-Doped Porous Carbon Nanofiber Webs for a Lithium−Sulfur Battery with High Capacity and Rate Performance. *J. Phys. Chem. C* **2014**, *118*, 1800−1807.